JAAS

Accepted Manuscript

This is an *Accepted Manuscript*, which has been through the Royal Society of Chemistry peer review process and has been accepted for publication.

Accepted Manuscripts are published online shortly after acceptance, before technical editing, formatting and proof reading. Using this free service, authors can make their results available to the community, in citable form, before we publish the edited article. We will replace this *Accepted Manuscript* with the edited and formatted *Advance Article* as soon as it is available.

You can find more information about *Accepted Manuscripts* in the Information for Authors.

Please note that technical editing may introduce minor changes to the text and/or graphics, which may alter content. The journal's standard Terms & Conditions and the Ethical guidelines still apply. In no event shall the Royal Society of Chemistry be held responsible for any errors or omissions in this *Accepted Manuscript* or any consequences arising from the use of any information it contains.

ROYAL SOCIETY OF CHEMISTRY

www.rsc.org/jaas

An approach of portable laser-induced breakdown spectroscopy based on a fiber laser with a background removal method was proposed.

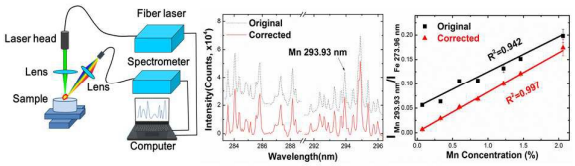

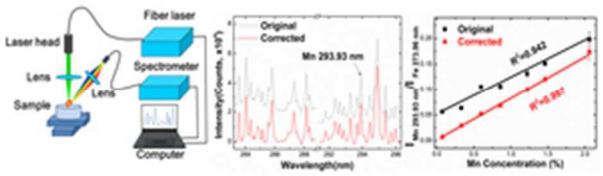

25x7mm (300 x 300 DPI)

Cite this: DOI: 10.1039/c0xx00000x

www.rsc.org/xxxxxx

ARTICLE TYPE

Quantitative Analyses of Mn, V, and Si Elements in Steels Using a Portable Laser-Induced Breakdown Spectroscopy System Based on a Fiber Laser

Qingdong Zeng,[a, b] Lianbo Guo,[a] Xiangyou Li,*[a] Meng Shen,[a] Yining Zhu,[a] Jiaming Li,[a] Xinyan Yang,[a] Kuohu Li,[a] Jun Duan,[a] Xiaoyan Zeng,[a] and Yongfeng Lu [a]

Received (in XXX, XXX) Xth XXXXXXXXX 20XX, Accepted Xth XXXXXXXXX 20XX
DOI: 10.1039/b000000x

A portable laser-induced breakdown spectroscopy (LIBS) system based on a fiber laser was developed and employed to quantitatively analyze manganese (Mn), vanadium (V), and silicon (Si) elements in steels. After background removal, the coefficients of determination (R^2 factors) of the calibration curves for Mn, V, and Si elements reached to 0.997, 0.991 and 0.992, respectively, obvious improvements compared to those of the original spectra. The leave-one-out cross-validation (LOOCV) method was used to test the system. The root-mean-square error of cross-validation (RMSECV) for Mn (0.072–2.06 wt.%) , V (0.009–0.821 wt.%), and Si (0.099–1.85 wt.%) elements were 0.037, 0.041 and 0.079 wt.%, respectively. The average relative errors (AREs) for Mn elements reached 7.6%. These results are comparable with the conventional LIBS which refers to utilizing the traditional flash-lamp-pumped laser as a laser source. However, compared to conventional LIBS, a fiber laser LIBS (FL-LIBS) is more compact, robust, and cost effective. The FL-LIBS, a coupling of a compact fiber laser and spectrometer, is a convenient approach to providing a portable solution for real-time and in situ detection in industry, especially in harsh environments.

1. Introduction

Minor elements in steels play an important role in their performance.[1-2] Traditional analyses of minor elements in steels are often carried out by complex analytical techniques, such as inductively coupled plasma (ICP) and X ray fluorescence (XRF), which are labor intensive and time consuming because they often need sample preparation, such as cutting, milling, grinding, and drilling. [3-5] Laser-induced breakdown spectroscopy (LIBS) is an appealing technique for elemental analyses in which a focused laser pulse ablates a sample while the spectral emission from the laser-induced plasmas is recorded and analyzed.[6-10] LIBS has been proven to be a versatile analytical technique in the past decades,[11-14] and has many advantages, including a high capability of multielement detection; little or no sample preparation, the ability to detect solid, liquid, and gas targets; and rapid and nearly nondestructive measurements.[14-17] However, traditional LIBS is limited when the environment is harsh or the access restriction makes it difficult to produce plasmas or acquire the emission lines[18-19] due to drawbacks such as large size, complex structure, cost, and robustness. Therefore, there is an urgent requirement to develop a portable, robust, and cost-effective LIBS system.

The laser is one of the most important parts of a portable LIBS system, and its size and performance influences the dimensions and capabilities of the overall instrument.[20] During past decades, great effort has been made to reduce the dimensions of the LIBS instrument with a goal of creating a portable application through the use of a compact flash-lamp-pumped solid state laser (FLPSS) and passively Q-switched microchips as laser sources.[20-29] However, there are still some attributes difficult to improve, but which can be crucial to maximum performance of the portable LIBS device.[20] Beam quality is one of those important parameters which are usually evaluated by the M^2 quantity. [20] Other problems for the compact laser are energy, jitter, and stability.

Recently, a fast-developing laser technology which seems to be very promising for LIBS application is the pulsed fiber laser.[30] With the advantages of higher photon conversion efficiency, high beam quality (M^2 factor close to 1), low cost, and compact size, the fiber laser has become more and more useful as it has grown in robustness, reliability, and peak power.[29-30] Moreover, with the ability to endure harsh environments, such as tolerance of dust, shock, and fluctuations in temperature and humidity, a fiber laser is a potential laser source for real-time and in situ LIBS in industry.

Until now, a fiber laser has not been widely used in LIBS; and only a couple of studies referring to fiber laser LIBS (FL-LIBS) have been reported. [20,29] Baudelet *et al.* [31] reported the first implementation of a 2 μm thulium fiber laser as the ablation source. The temperature and electron density were calculated, and the plasma was proven to be in the local thermodynamic equilibrium. They claimed that the fiber laser had the potential to

greatly accelerate the improvement and enable the development of a new generation of LIBS systems by utilizing rugged, compact, and efficient fiber laser systems.[31] Gravel *et al.*[29] evaluated the potential of a pulsed fiber laser source for LIBS application coupled with three different detection systems, and they demonstrated the fiber laser's capabilities for elemental analysis of aluminum and copper alloys. Huang *et al.* [32] first evaluated the LIBS studies on elemental composition detection and identification using a 1030 nm femtosecond (fs) fiber laser and the performance of an intensified charge-coupled device (ICCD) system and a nonintensified CCD system were also compared. Scharun *et al.* [33] reported a multi-kHz fiber-laser-based LIBS setup for mobile metal analysis tasks. The accuracy they achieved was similar to or even better than the mobile spark discharge optical emission spectroscopy (SD-OES) apparatus under the described concentration ranges and measurement conditions.

The aforementioned works provided versatile solutions and obtained good results for the LIBS application. However, it is difficult to avoid continuum background influence of spectra in a portable FL-LIBS system using a compact spectrometer (coupled with a CCD detector) due to the high pulse repetition frequency (PRF) of the fiber laser. (The CCD system spectrometer was chosen in this work because it was more compact, robust, and inexpensive than an ICCD system spectrometer.[34]) The continuum background, which is generated by the bremsstrahlung radiation, recombination radiation, and stray lights, [35] would influence the analytical results. The precision and sensitivity of LIBS can be improved by enhancing the signal strength or reducing the background.[36,37] Some methods have been proposed to eliminate continuum background in conventional LIBS (Sun *et al.*,[38] Yuan *et al.*,[39] and Zou *et al.*[40]). However, in a portable FL-LIBS system, the continuum background is quite different from the conventional flash-lamp-pumped laser. The background is diverse and very intense because it is an accumulation of hundreds of shots over an integration time due to the multi-kHz repetition rates of the laser. There have been few research studies on the qualitative and quantitative analyses before and after background correction in a portable FL-LIBS system.

In this work, a portable FL-LIBS system, coupling a compact fiber laser with a spectrometer, was developed. Qualitative and quantitative analyses of Mn, V, and Si elements in steels were carried out with background correction in this FL-LIBS system. The leave-one-out cross-validation method was used to evaluate the accuracy of the quantitative analyses.

2. Experimental setup and methodology

2.1 Experimental setup

A schematic diagram of the FL-LIBS setup is shown in Figure 1. A compact Ytterbium-doped pulsed fiber laser model YDFLP-20-PRO-S (Shenzhen JPT Electronics Co., Ltd., China, size: 31×22×10 cm) based on the Master Oscillator Power Amplifier (MOPA) configuration, with an average power of 20 W and wavelength of 1064±3 nm (emission bandwidth: full width at half maximum (FWHM) <10 nm) was employed. The peak power of laser can be varied from 9–13 kW depending on the pulse duration (10–200 ns). The repetition rates can be varied from 25–400 kHz, and maximum pulse energies are up to 0.4 mJ. The output of the fiber laser is coupled to a laser head (size: ϕ3.5×23 cm, consisting of the fiber collimator, the optical isolator, and the beam expander), which produces a low divergence beam of 7 mm diameter. This beam is focused by a plano-convex lens of 100 mm focal length onto the target at normal incidence.

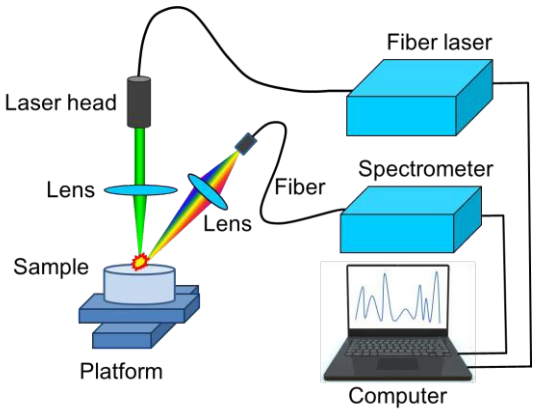

Fig. 1. Schematic diagram of FL-LIBS system.

The plasma light emission was collected by a compact time-integrated spectrometer (size: 17×10.5×4.5 cm), which was a single-channel, ultralow, stray light fiber optic spectrometer (AvaSpec-ULS2048L-PURGE, Czerny-Turner, grating: 2400 lines/mm, slit: 10 μm). The covered spectral range was from 193 nm to 299 nm with an optical resolution of approx. 0.08–0.11 nm depending on the wavelength. The spectrometer was coupled with a gated linear CCD detector with 2048 elements, and the minimum integration time was 1.1 ms. A computer-controlled platform was used to move the samples. The processing parameters were optimized and fixed as follows. The pulse duration of the laser was set to 10 ns, and the repetition rate was fixed at 100 kHz, generating a high peak power of approximate 13 kW. The lens to sample distance (LTSD) was 99 mm to obtain the best LIBS signal with high intensity and signal-to-background ratio (S/B). In the present work, a 2 ms integration time was used. With a repetition rate of 100 kHz, 2 ms of data collection results in an integration of 200 consecutive laser-generated plasmas in every acquisition. Every measurement in the experiment was repeated ten times unless otherwise specified, and each spectrum was averaged ten times. Both the laser and the spectrometer, as well as their timing sequence, were controlled by a computer.

2.2 Method of background correction

Wavelet transform (WT) is a signal processing technique with the capability for signal decomposition.[36] Generally, a given signal f (t) can be expanded to the linear combination of a series of wavelet bases.[41] The spectra usually contain three main types of frequency information: high frequency (noise), low frequency (background), and medium frequency (peaks).[40-43] The basic idea of background removal is to remove the low-frequency part of the spectra.

In this work，an algorithm of background removal based on wavelet transform was adopted. The samples were classified into two groups: one group as training set and another group as test set. The main procedures of the background correction were as follows:

(1) Read the data of spectra to software.
(2) Optimize parameters from the training set.
Determine the optimum parameters [wavelet function (W), decomposition level (L), and scale factor γ)], which makes the root-mean-square error of calibration (RMSEC) of analyzed element achieve the minimum. [40]
(3) Remove the background for the samples in the test set using wavelet transform with the optimum parameters. [40]
(4) Output the data of background-corrected spectra on the computer.

2.3 Samples

Six certified carbon steel samples (GBW01211-01216, Fushun Steel Shares Co., Ltd.) were used for parameters optimization of wavelet transform (training set). Seven certified pig iron samples (GSB 03-2582-2010 series) purchased from Pangang Group Research Institute Co., Ltd. were used for background removal and quantitative analyses (test set) in this work. The matrix elements in all of these samples were iron with a content of over 90%. The concentrations of the Mn, V, and Si elements are listed in Table 1 and Table 2.

Table 1 Reference concentrations of Mn, V, and Si elements in the pig iron samples (wt.%).

	Concentration by Sample No.						
Ele-ment	1-1	1-2	1-3	1-4	1-5	1-6	1-7
Mn	0.072	0.329	1.22	0.857	0.596	1.46	2.06
V	0.009	0.044	0.071	0.158	0.335	0.506	0.821
Si	0.099	0.183	0.451	0.689	0.937	0.99	1.85

Table 2 Reference concentrations of Mn, V, and Si elements in the carbon steel samples (wt.%).

	Concentration by Sample No.					
Element	2-1	2-2	2-3	2-4	2-5	2-6
Mn	0.712	0.342	1.02	0.058	1.27	0.226
V	0.108	0.063	0.172	0.242	0.049	0.286
Si	0.282	0.368	0.189	0.031	0.517	0.133

3. Results and discussion

3.1 Qualitative analyses

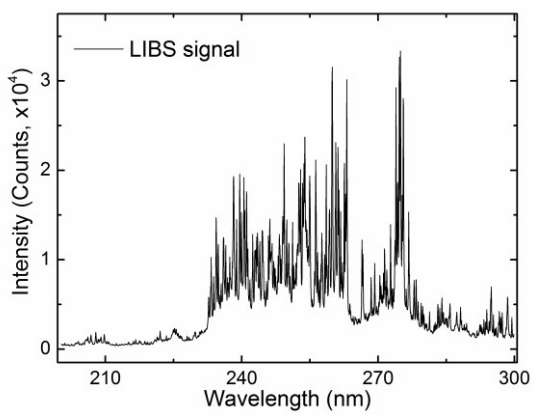

Fig. 2. The LIBS spectra of the sample No.1-6 acquired by the portable FL-LIBS system

Figure 2 shows the LIBS spectra that were acquired using the portable FL-LIBS system. Obviously, there existed an intense continuum background in the spectra, which was generated by the major bremsstrahlung emission mechanism predominating in the early plasma.[7] Due to the high repetition rates of the fiber laser and the integration time of the compact spectrometer, it was difficult to avoid continuous background by time delay because there were 200 consecutive laser-generated plasmas in an integration time. Therefore, the continuum background and the line radiation were accumulated together 200 times. This is the reason why the continuum background was strong. Background existence in spectra would disturb the true intensity of line radiation, which would lead to an inaccuracy in detection. Using the method of background removal based on wavelet transform, the spectra were corrected as shown in Figure 3. Obviously, the background of the spectra after the correction was lower than the original spectra.

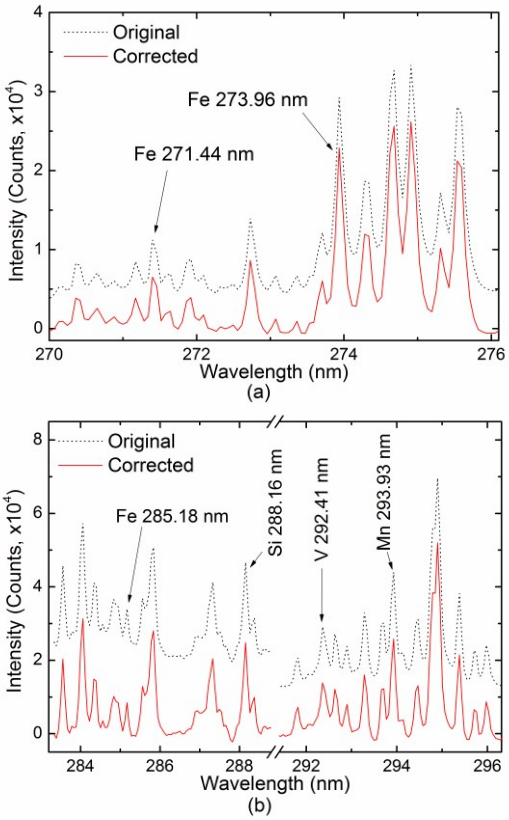

Fig. 3. The characteristic spectra of matrix Fe (a), Mn, V, and Si elements (b) of the sample No.1-6 in the portable FL-LIBS system.

The characteristic emission lines of Mn, V, and Si elements of matrix Fe are shown in Figure 3. There is almost no obvious difference in the shape of the spectral line before and after background correction except in the intensity. However, the background was clearly lower after the disposal of background correction. In addition, the signal to background ratio (SBR) was obviously improved after background removal. For example, the SBR for line Mn 293.93 nm was improved from 3.2 to 28.6, with the spectral range 291.32–291.66 nm as the background/noise area. The signal to noise ratio (SNR) keeps constant because the noise hadn't been changed.

3.2 Quantitative analyses

In LIBS, elemental concentration is determined by the peak intensities of the spectra. A calibration curve obtained from materials of known composition is used to determine the concentration of a substance in an unknown sample, by comparing the unknown with a set of standard samples of known concentration.[6,7,14] In this work, the internal standardization was adopted as the quantitative analysis method, which used intensity ratios (analyte/reference) to construct the calibration curve instead of absolute peak heights. This method has many advantages, such as minimizing shot-to-shot variations in the LIBS emission signal, increasing measurement precision, and correcting nonlinear behavior in calibration curves.[7, 14]

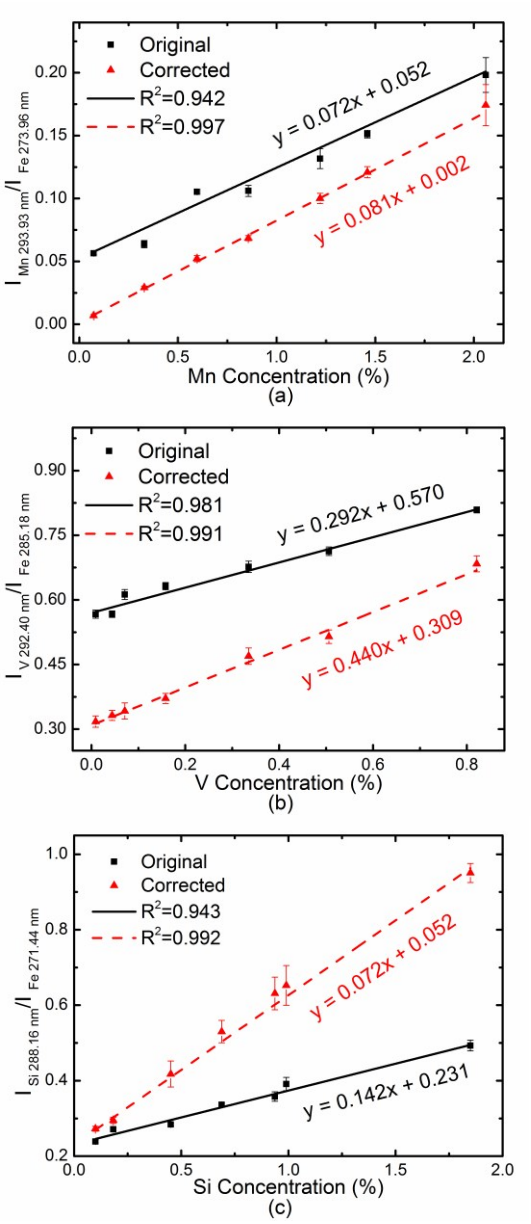

Fig. 4. Calibration curves for intensity ratios of (a) Mn 293.931 nm/ Fe I 273.96 nm, (b) V 292.40 nm/ Fe 285.18 nm, and (c) Si 288.16 nm/ Fe 271.44 nm in the pig iron samples before and after background correction.

Consideration of little or no self-absorption and interference, the spectrum lines of Mn 293.93 nm, V 292.40 nm, and Si 288.16 nm were chosen as the analytical spectral lines. The matrices Fe 273.96 nm, Fe 271.44 nm, and Fe 285.18 nm were adopted as the reference lines for Mn 293.93 nm, V 292.40 nm, and Si 288.16 nm, respectively.

Quantitative analyses of Mn, V, and Si elements in the pig iron samples were carried out using the FL-LIBS system. The calibration curves for intensity ratios of Mn 293.931 nm/Fe I 273.96 nm, V 292.40 nm/Fe 285.18 nm, and Si 288.16 nm/Fe 271.44 nm were established and shown in Figure 4 (a), 4(b), and 4(c), respectively. The coefficients of determination (R^2 factors) of the calibration curves and the limit of detection (LOD) were calculated and listed in Table 3. As shown in Fig. 4, the R^2 factors of the calibration curves were all improved after background correction. It was probably due to the removal of the continuum background, which influences the true intensity of spectra.

The leave-one-out cross-validation (LOOCV) method was utilized to evaluate the accuracy of detection. In the LOOCV method, the n−1 samples were used to establish the calibration curve; and the remaining sample was used as the test sample. Each sample was tested in turn. The root means square error of cross-validation (RMSECV) was used as the main index for evaluating the performance of the system. The RMSECV is calculated by [6, 44]

$$RMSECV = \sqrt{\frac{\sum_{i=1}^{n}(x_i - \hat{x}_i)^2}{n}}, \quad (1)$$

where $\hat{x}_i$ is the reference concentration of the sample, x_i is the predicted concentration of the sample, and n is the number of samples. According to Eq (1), the RMSECVs for Mn, V, and Si elements before and after background correction in FL-LIBS systems were calculated and are listed in Table 3. The average relative standard deviations (ARSDs) were also listed in Table 3. In addition, the relative errors (REs) and average relative errors (AREs) for each sample using the LOOCV method were calculated and listed in Table 4.

As shown in Table 3, both the R-square (R^2) factors and the RMSECV improved after background correction; and the values reached to 0.997 and 0.037 wt.% for the Mn element. However, the LODs and the ARSDs were slightly inferior after background correction. This was ascribed to the reduction of the intensity of the spectral line. The RSD is the ratio of standard deviation (SD) and the average value, and the standard deviation (SD) was nearly invariable for a spectrum line before and after background correction. When the average value was decreased due to the reduction of the intensity of the spectra line, the RSD increased. The LODs are slightly inferior to the conventional LIBS, probably due to the low ablation energy (up to 0.4 mJ per pulse). As shown in Table 4, most of the values of REs and AREs were improved after background correction, especially for the Mn element; and the AREs reached to 7.6%. These results are comparable to the previous studies of conventional LIBS [6,7,10,13] and slightly better than most of the portable LIBS systems reported previously.[20-29,45]

Table 3. The ARSDs, R-square (R^2) factors, RMSECVs (wt.%), and LODs for Mn, V, and Si elements before and after background correction in the FL-LIBS system.

Spectral line	ARSD (%)		R^2		RMSECV(wt.%)		LOD (ppm)	
(analyte/reference)	Original	Corrected	Original	Corrected	Original	Corrected	Original	Corrected
Mn 293.93/Fe273.96	3.9	6.0	0.942	0.997	0.152	0.037	165	195
V 292.40/Fe 285.18	1.5	3.7	0.981	0.991	0.056	0.041	32	48
Si 288.16/Fe 271.44	2.4	5.3	0.943	0.992	0.099	0.079	69	110

Table 4. The REs and AREs for Mn, V, and Si elements using the LOOCV method before and after background correction in the FL-LIBS system.

Mn			V			Si		
C^*(wt.%)	RE (%)		C^*(wt.%)	RE (%)		C^*(wt.%)	RE (%)	
	Original	Corrected		Original	Corrected		Original	Corrected
0.072	124.983	32.182	0.009	291.965	157.587	0.099	96.378	19.967
0.329	58.287	5.179	0.044	201.616	24.594	0.183	74.752	16.816
0.596	36.596	5.454	0.071	118.691	5.473	0.451	23.678	4.955
0.857	14.279	5.358	0.158	41.316	14.350	0.689	10.894	10.706
1.22	10.455	0.452	0.335	9.718	9.689	0.937	5.754	8.637
1.46	13.173	1.146	0.506	4.03	10.716	0.99	14.448	8.091
2.06	1.991	3.578	0.821	3.17	10.319	1.85	1.018	8.308
ARE	37.109	7.621		95.786	33.247		32.417	11.069

* the concentration of the analyzed element.

4. Conclusions

In summary, a portable FL-LIBS system based on a fiber laser and a compact spectrometer was developed for quantitative analyses of Mn, V, and Si elements in steels. After background correction, the R^2 factors for Mn, V, and Si elements reached to 0.997, 0.991 and 0.992, respectively. The RMSECVs for Mn, V, and Si elements were 0.037, 0.041 and 0.079 wt.%, respectively; and the AREs reached 7.6 % for Mn elements. These results were comparable to the previous studies of conventional LIBS and slightly better than most of the portable LIBS systems reported previously. Furthermore, the FL-LIBS, coupling a compact fiber laser and a spectrometer, provides a convenient approach to a portable solution for the application of LIBS to industry, with the advantages of being compact, robust, and cost effective.

Acknowledgement

This research was financially supported by the National Special Fund for the Development of Major Research Equipment and Instruments (No. 2011YQ160017), the National Natural Science Foundation of China (No. 61575073, 51429501, and 61378031) , and the Fundamental Research Funds for the Central Universities (HUST: 2015TS075).

Notes and references

[a] *Wuhan National Laboratory for Optoelectronics (WNLO), Huazhong University of Science and Technology (HUST), Wuhan, Hubei 430074, P.R. China. Fax: 86-27-87541423; Tel: 86-27-87541423; E-mail: xyli@mail.hust.edu.cn*

[b] *School of Physics and Electronic-information Engineering, Hubei Engineering University, Xiaogan 432000, P.R. China.*

1. M.-A. Van Ende, M. Guo, P. T. Jones, B. Blanpain and P. Wollants, ISIJ Int., 2008, 48, 1331-1338. DOI: 10.2355/isijinternational.48.1331.
2. H. Suito and R. Inoue, ISIJ Int., 1995, 35, 266-271. DOI: 10.2355/isijinternational.35.266.
3. V. Sturm, J. Vrenegor, R. Noll and M. Hemmerlin, *J. Anal. At. Spectrom.*, 2004, 19, 451-456.
4. V. Sturm, L. Peter and R. Noll, *Applied Spectroscopy*, 2000, 54, 1275-1278.
5. V. Sturm, R. d. Fleige, M. de Kanter, R. Leitner, K. Pilz, D. Fischer, G. Hubmer and R. Noll, *Analytical chemistry*, 2014, 86, 9687-9692.
6. R. Noll, *Laser-Induced Breakdown Spectroscopy*, Springer. 2012.
7. J. P. Singh and S. N. Thakur, *Laser-induced breakdown spectroscopy*, Elsevier. 2007.
8. O. A. Nassef and H. E. Elsayed-Ali, *Spectrochimica Acta Part B: Atomic Spectroscopy*, 2005, 60, 1564-1572.
9. D. A. Cremers and R. C. Chinni, *Applied Spectroscopy Reviews*, 2009, 44, 457-506.
10. Z. Wang, T.-B. Yuan, Z.-Y. Hou, W.-D. Zhou, J.-D. Lu, H.-B. Ding and X.-Y. Zeng, *Frontiers of Physics*, 2014, 9, 419-438. DOI: 10.1007/s11467-013-0410-0.
11. J. Yu and R. Zheng, *Frontiers of Physics*, 2012, 7, 647-648. DOI: 10.1007/s11467-012-0275-7.
12. F.-Z. Dong, X.-L. Chen, Q. Wang, L.-X. Sun, H.-B. Yu, Y.-X. Liang, J.-G. Wang, Z.-B. Ni, Z.-H. Du, Y.-W. Ma and J.-D. Lu, *Frontiers of Physics*, 2012, 7, 679-689. DOI: 10.1007/s11467-012-0263-y.
13. Q. Zeng, L. Guo, X. Li, C. He, M. Shen, K. Li, J. Duan, X. Zeng and Y. Lu, *J. Anal. At. Spectrom.*, 2015, 30, 403-409. DOI: 10.1039/C4JA00462K.
14. D. W. Hahn and N. Omenetto, *Applied Spectroscopy*, 2012, 66, 347-419.
15. L. Guo, B. Zhang, X. He, C. Li, Y. Zhou, T. Wu, J. Park, X. Zeng and Y. Lu, *Optics express*, 2012, 20, 1436-1443.
16. L. Liu, S. Li, X. He, X. Huang, C. Zhang, L. Fan, M. Wang, Y. Zhou, K. Chen and L. Jiang, *Optics express*, 2014, 22, 7686-7693.
17. Z. Wang, F. Z Dong and W. D. Zhou, Plasma Science and Technology, 2015, 617-620.
18. G. A. Theriault, S. Bodensteiner and S. H. Lieberman, *Field Analytical Chemistry & Technology*, 1998, 2, 117-125.
19. F. Anabitarte, A. Cobo and J. M. Lopez-Higuera, *ISRN Spectroscopy*,

2012, 12. DOI: 10.5402/2012/285240.
20. J. Rakovský, P. Čermák, O. Musset and P. Veis, *Spectrochimica Acta Part B: Atomic Spectroscopy*, 2014, 101, 269-287. DOI: http://dx.doi.org/10.1016/j.sab.2014.09.015.
21. K. Y. Yamamoto, D. A. Cremers, M. J. Ferris and L. E. Foster, Applied Spectroscopy, 1996, 50, 222-233.
22. J. Cuñat, F. J. Fortes and J. J. Laserna, *Analytica Chimica Acta*, 2009, 633, 38-42. DOI: http://dx.doi.org/10.1016/j.aca.2008.11.045.
23. J. Rakovský, O. Musset, J. Buoncristiani, V. Bichet, F. Monna, P. Neige and P. Veis, Spectrochimica Acta Part B: Atomic Spectroscopy, 2012, 74–75, 57-65. DOI:10.1016/j.sab.2012.07.018
24. E. Hondrogiannis, D. Andersen, A.W. Miziolek, SPIE Def. Secur. Sens. 8726 (2013) 87260P, http://dx.doi.org/10.1117/12.2017900.
25. C. Lopez-Moreno, K. Amponsah-Manager, B. W. Smith, I. B. Gornushkin, N. Omenetto, S. Palanco, J. J. Laserna and J. D. Winefordner, J. Anal. At. Spectrom., 2005, 20, 552–556.
26. G. Cristoforetti, S. Legnaioli, V. Palleschi, A. Salvetti, E. Tognoni, P. Alberto Benedetti, F. Brioschi and F. Ferrario, J. Anal. At. Spectrom., 2006, 21, 697–702.
27. K. Amponsah-Manager, N. Omenetto, B. W. Smith, I. B. Gornushkin and J. D. Winefordner, J. Anal. At. Spectrom., 2005, 20, 544–551.
28. J. Wormhoudt, F. J. Iannarilli,Jr, S. Jones, K. D. Annen and A. Freedman, Appl. Spectrosc., 2005, 59, 1098–1102.
29. J.-F. Gravel, F. Doucet, P. Bouchard and M. Sabsabi, *J. Anal. At. Spectrom.*, 2011, 26, 1354-1361.
30. S. Musazzi and U. Perini, *Laser-Induced Breakdown Spectroscopy: Theory and Applications*, Springer. 2014.
31. M. Baudelet, C. C. Willis, L. Shah and M. Richardson, *Optics Express*, 2010, 18, 7905-7910.
32. H. Huang, L.-M. Yang and J. Liu, *Appl. Optics*, 2012, 51, 8669-8676.
33. M. Scharun, C. Fricke-Begemann and R. Noll, *Spectrochimica Acta Part B: Atomic Spectroscopy*, 2013, 87, 198-207.
34. H. Heilbrunner, N. Huber, H. Wolfmeir, E. Arenholz, J. Pedarnig and J. Heitz, *Spectrochimica Acta Part B: Atomic Spectroscopy*, 2012, 74, 51-56.
35. T. Fujimoto, *Plasma Spectroscopy* (Clarendon, 2004).
36. B. Zhang, L. Sun, H. Yu, Y. Xin and Z. Cong, Spectrochimica Acta Part B: Atomic Spectroscopy, 2015, 107, 32-44. DOI: http://dx.doi.org/10.1016/j.sab.2015.02.015.
37. L. Sun, H. Yu, Z. Cong, Y. Xin, Y. Li and L. Qi, Spectrochimica Acta Part B: Atomic Spectroscopy, 2015, 112, 40-48. DOI: http://dx.doi.org/10.1016/j.sab.2015.08.008.
38. L. Sun and H. Yu, *Spectrochimica Acta Part B: Atomic Spectroscopy*, 2009, 64, 278-287. DOI: http://dx.doi.org/10.1016/j.sab.2009.02.010.
39. T. Yuan, Z. Wang, Z. Li, W. Ni and J. Liu, *Analytica Chimica Acta*, 2014, 807, 29-35. DOI: http://dx.doi.org/10.1016/j.aca.2013.11.027.
40. X. Zou, L. Guo, M. Shen, X. Li, Z. Hao, Q. Zeng, Y. Lu, Z. Wang and X. Zeng, *Optics express*, 2014, 22, 10233-10238.
41. S. G. Mallat, A Wavelet Tour of Signal Processing: The Sparse Way (Academic, 2008).
42. C. Galloway, E. Le Ru and P. Etchegoin, *Applied spectroscopy*, 2009, 63, 1370-1376.
43. J. Zhao, H. Lui, D. I. McLean and H. Zeng, *Applied spectroscopy*, 2007, 61, 1225-1232.
44. S. Yao, J. Lu, M. Dong, K. Chen, J. Li and J. Li, *Applied spectroscopy*, 2011, 65, 1197-1201.
45. A. Freedman, F. J. Iannarilli Jr and J. C. Wormhoudt, *Spectrochimica Acta Part B: Atomic Spectroscopy*, 2005, 60, 1076-1082. DOI: http://dx.doi.org/10.1016/j.sab.2005.03.020.